Ratio of entropy to enthalpy in thermal transitions in biological tissues

Steven L. Jacques
Oregon Health and Science University
Departments of Dermatology and
Biomedical Engineering
20000 NW Walker Road
Beaverton, Oregon 97006
E-mail: sjacques@bme.ogi.edu

Abstract. Thermal transitions in biological tissues that have been reported in the literature are summarized in terms of the apparent molar entropy (ΔS) and molar enthalpy (ΔH) involved in the transition. A plot of ΔS versus ΔH for all the data yields a straight line, consistent with the definition of free energy, $\Delta G = \Delta H + T\Delta S$. Various bonds may be involved in cooperative bond breakage during thermal transitions; however, for the sake of description, the equivalent number of cooperative hydrogen bonds can be cited. Most of the tissue data behave as if 10 to 20 hydrogen bonds are cooperatively broken during coagulation, with one transition, the expression of heat shock protein, involving 90 cooperative hydrogen bonds. The data are consistent with $\Delta S = a + b\Delta H$, where $a = -327.5$ J/(mol K) and $b = 31.47 \times 10^{-4}$ K^{-1}. If each additional hydrogen bond adds 19×10^3 J/mol to ΔH, then each additional bond adds 59.8 J/(mol· K) to ΔS. Hence, the dynamics of irreversible thermal transitions can be described in terms of one free parameter, the apparent number of cooperative hydrogen bonds broken during the transition. [DOI: 10.1117/1.2343437]

Keywords: thermal effects; x ray; x ray lasers.

Paper 05311SSR received Oct. 13, 2005; revised manuscript received May 1, 2006; accepted for publication May 1, 2006; published online Sep. 8, 2006.

1 Introduction

In the early years of biomedical optics, the interactions of lasers and light with biological tissues were first being explored. In the late 1970s and early 1980s, people were zapping tissues with lasers and examining biopsies to see what had happened. Investigators were working to lay the foundations for understanding the interactions of lasers and light with tissues. Professor Welch at the University of Texas at Austin was one of the early investigators defining the photochemical, photothermal, and photomechanical effects of laser exposures. For this special issue dedicated to Welch, this report will revisit the topic of thermal damage to tissues, in which Welch conducted research, trained students, and had significant impact during the formative years of our field.

Thermal coagulation of tissues is sometimes a desired therapeutic effect, such as when coagulating a tumor using a laser, and sometimes causes unwanted damage, such as the collateral injury to normal tissue adjacent to the targeted tumor. Thermal curing can be a desired procedure in the fabrication of a biomaterial structure. For a variety of reasons, a biomedical optical engineer is occasionally faced with the need to estimate the time-temperature exposure that will cause a thermal transition. Biological materials present a range of thermal transition properties, ranging from the slow low-temperature exposures that can inactivate thermally labile enzymes to the fast high-temperature exposures required to coagulate collagen fiber bundles. Despite the variety of thermal transitions encountered, most irreversible thermal transitions involve simultaneous cooperative breakage of many bonds. A variety of bonds may be involved (van der Waals, hydrogen, ionic, disulfide, covalent) in thermal transitions, and the rate of such transitions is characterized by the number of bonds being cooperatively broken.

This paper summarizes published literature values on the thermal coagulation properties of various thermal transitions experimentally observed. The relationship between the molar entropy, ΔS [J/(mol·K)], and the molar enthalpy, ΔH [J/mol], of such transitions is explored. Such irreversible thermal transitions in tissues include changes in optical scattering, mechanical contraction, loss of birefringence and delayed necrosis seen two days after thermal exposure.

2 The Basics of Thermal Damage

Consider a native form molecule (N) that can be converted to a denatured form (D) (see Fig. 1). There is an energetic barrier to such a conversion. The Arrhenius rate process description of irreversible thermal damage describes the process in terms of a rate [A (s^{-1})] at which the native form molecule moves to a transition state (N^*) atop an energy barrier, $N \rightarrow N^*$, and a probability ($\exp[-E/(RT)]$ [dimensionless]) that the molecule will convert from the transition state to the denatured state, $N^* \rightarrow D$. The symbol E denotes the activation energy (J/mol) for the conversion. The factor R is the gas constant [8.314 J/(mol·K)]. The T is temperature expressed

Address all correspondence to Steven Jacques, Biomedical Engineering/Dermatology, Oregon Health & Science Univ., 20000 NW Walker Rd., Beaverton, OR 97006; Tel: 503-748-1512; Fax: 503-748-1406; E-mail: sjacques@bme.ogi.edu

1083-3668/2006/11(4)/041108/7/$22.00 © 2006 SPIE

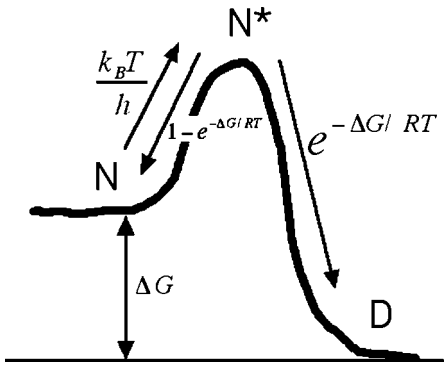

Fig. 1 A native state molecule (N) moves to a transition state (N^*) at a rate specified by $k_BT/h(s^{-1})$ then either returns to the native state or converts to an irreversibly denatured form (D). The free energy of the transition from N to D is ΔG (J/mol).

in Kelvin ($T=273.15+T_{\circ C}$). The rate of conversion, $k(s^{-1})$, from N to D is given by the expression

$$k = Ae^{-E/(RT)} \tag{1}$$

If the initial number of native molecules is N_o, then the number of surviving native molecules as a function of time is

$$N(t) = N_o e^{-\Omega(t)}, \tag{2}$$

where

$$\Omega(t) = \int_0^t k(t')\mathrm{d}t'. \tag{3}$$

The factor Ω is called the damage integral, which extends from 0 to ∞, such that $N(t)$ falls from N_o to 0. At any time, the number of denatured molecules, $D(t)$, equals the difference $N_o - N(t)$.

The above formalism using A and E can be alternatively expressed in terms of the molar entropy, ΔS [J/(mol K)], and the molar enthalpy, ΔH(J/mol). The free energy, ΔG (J/mol), associated with the transition from the native to denatured form specifies the probability $\exp[-\Delta G/(RT)]$. The free energy is related to ΔS and ΔH

$$\Delta G = \Delta H - T\Delta S. \tag{4}$$

By convention, the rate at which molecules move from the native state N to the transition state N^* is assigned the value k_BT/h, where k_B is the Boltzmann constant (1.381×10^{-23} J/K) and h is Planck's constant (6.626×10^{-34} J·s). This rate is 6.2×10^{12} s^{-1} at room temperature. It should be emphasized that this is a convention, and the value of ΔS is reliant on this assumption regarding the frequency of the transition $N \rightarrow N^*$. Using this convention, the probability of transition is

$$k = \frac{k_B T}{h} e^{\Delta S/R} e^{-\Delta H/(RT)}. \tag{5}$$

The values for A and E that characterize a thermal coagulation process are experimentally specified in experiments in which the rate of coagulation (k) as a function of exposure time (t) and exposure temperature (T) are determined.

The parameters A and E of Eq. (1) are related to the ΔS and ΔH of Eq. (5)

$$A = \frac{k_B T}{h} e^{\Delta S/R},$$

$$E = \Delta H. \tag{6}$$

Although the convention that the native molecules sample the transition state N^* at a rate k_BT/h is fraught with assumption, the convention suggests that this rate of sampling is proportional to temperature. In contrast, using A to interpret experimental data assumes the sampling is independent of temperature. Note that the value of $\ln(k_BT/h)$ varies over 27.4 to 29.8 for T in the 40 to 140 °C range. This temperature dependence of the sampling frequency is not strong because the modest range of temperature variation in most experiments results in only a moderate change in temperature on the Kelvin scale (0 to 100 °C equals 273 to 373 K). The value of A is influenced more by the ΔS in the exponential term $\exp(-\Delta S/R)$ than by the linear dependence on temperature in the term k_BT/h. So whether one interprets experimental data in terms of A and E, or in terms of ΔS and ΔH, one gets about the same answer. The important lesson from Eq. (5) [or Eq. (1)] is that the temperature-dependent component of k is determined by ΔH (or E) and that the relatively temperature-independent component of k is determined by ΔS (or A).

Experimentally, coagulation is observed to proceed as a first-order process with the following form, in which an observed parameter X is measured throughout a time period t of exposure to a constant temperature that determines the rate constant k

$$X(t) = X(0) + [X(\infty) - X(0)][1 - \exp(-kt)]. \tag{7}$$

The parameter X starts at an initial value $X(0)$ and proceeds exponentially toward a final stable value $X(\infty)$. Analysis of the measured values of $X(t)$ yields the rate constant k for a given temperature T. Repeating the experiment for different values of T yields the temperature dependence of k.

A typical experiment might involve wrapping a thin tissue slice in aluminum foil to keep its hydration constant, then immersing the tissue in a hot water bath at a known temperature for a variable amount of time. After the allotted time, the tissue is removed and an experimental measurement is made that is sensitive to the degree of biomolecular aggregation that follows denaturation and constitutes "irreversible coagulation". There are a variety of transitions that can be monitored to indicate coagulation, for example, loss of collagen birefringence observed through a polarizing microscope, loss of enzyme activity, histologic evidence of necrosis seen two days after thermal exposure, and changes in optical scattering. With regard to optical changes, the coagulation of egg white and the whitening of soft tissues such as muscle or liver during cooking involves denaturation and aggregation of proteins into light-scattering aggregates. The denaturation of collagenous tissue to yield gelatin involves the partial loss of the collagen fiber bundle structure to yield a reduced-scattering material.

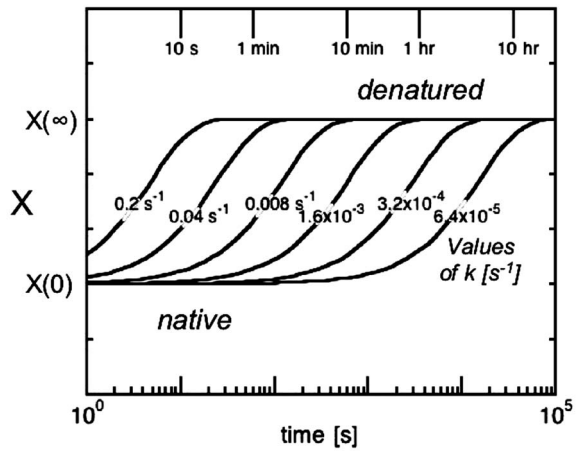

Fig. 2 Time course of irreversible coagulation process for various rate constants, $k(s^{-1})$. The x axis is the time of exposure at a constant temperature and hence at a constant k. The y axis is a generic linear measurement, X, of the degree of denaturation [measuring $X(0)$ for native biomaterial, and $X(\infty)$ for denatured biomaterial]. As the temperature of the water bath decreases, the value of the rate constant k decreases from 0.2 s^{-1} to 6.4×10^{-5} s^{-1}, and the process of complete denaturation increases from 10 s to 10 h.

Figure 2 shows the generic time course for irreversible denaturation with various rate constants k. The thermal transition shown is a generic transition proceeding from a native form to a denatured form. A measurement $X(t)$ starts at $X(0)$ for native biomaterial and completes at $X(\infty)$ for denatured biomaterial. While the transition is displayed as an increase in the y-axis value X for progression from native to denatured, for example, as scattering increases in a tissue during thermally induced whitening, the figure could just as easily be displayed as a decrease in the y-axis value, for example, as a loss of birefringence due to thermal denaturation. The curves in Fig. 2 are for various values of k. Recall that k (s^{-1}) equals 1/(time of exposure) at constant temperature required to achieve $1-1/e$ or 63% completion of an irreversible thermal transition. As the temperature decreases, k decreases and the time required for complete coagulation increases. On a linear time scale, these curves are obvious exponentials. On a logarithmic time scale, the curves look like sigmoids, which slide on the time scale as k is varied but do not change their shape.

3 Summary of Experimental Results from Literature and Unpublished Work

Typical values of ΔS and ΔH for examples of thermal coagulation are listed in Table 1 (Refs. 1–3). References 1–3 are from Welch's laboratory. If data were reported as A and E, then ΔH was set to E and the A was converted to ΔS assuming $T=50\,^{\circ}\mathrm{C}$ and using Eq. (6). As mentioned above, this assumption of $T=50\,^{\circ}\mathrm{C}$ is not critical to the final value of ΔS. Using Eq. (4), the values of ΔS and ΔH in Table 1 typically yield a value of ΔG equal to about 100×10^3 J/mol for the thermal transition over the range of 40 to $80\,^{\circ}\mathrm{C}$.

The rate constant k for each example varies as a function of temperature. It is common to consider the exposure time t_Ω (s) required to achieve $\Omega=1$, which corresponds to exposure time $t_\Omega=1/k$, as a function of the temperature. Figure 3 plots the threshold exposure time versus exposure temperature curves for the several examples of coagulative transitions in Table 1. Each line serves as the threshold for coagulation. For example, at a given exposure temperature as the exposure time increases, one crosses the threshold from the lower left region labeled "no effect" into the upper right region labeled as "coagulation". Similarly, at a given exposure time, increasing the exposure temperature causes one to cross the line from "no effect" into the "coagulation" region. The more structured the structure being coagulated, the more bonds that must be cooperatively broken to achieve coagulation, and the more vertical is the threshold curve. The larger magnitude of entropy (ΔS) and enthalpy (ΔH) in the exponents of Eq. (5) leads to a sharper transition. An extreme example would be a crystal, which would be portrayed as a vertical line at the melting temperature of the crystal. The less structured the molecular structure to be denatured, the more horizontal is the curve since the magnitudes of ΔS and ΔH are lower.

4 Common Energetics of Experimental Data

Figure 4 plots the ΔS versus ΔH for all the thermal transitions in Table 1. The experimental data suggest that the entropy ΔS released by denaturation of a molecular structure involved in an irreversible thermal transition is to a first approximation linearly related to the enthalpy ΔH of the transition. This interpretation is consistent with the definition of ΔG in Eq. (4) if the types of bonds being broken involve a common incremental order asserted per unit enthalpic bond energy. Although several types of bonds may be involved in cooperative bond breakage, the constant ratio suggests that a convenient convention can be used for simple description, that is the equivalent number of hydrogen bonds being cooperatively broken during a transition. Hydrogen bonds are common in stabilizing proteins and other biomolecules, therefore the hydrogen bond is used for this convention. Figure 4 shows a linear fit to the ΔS versus ΔH data, based on transitions 1 to 22 shown as circles, but excluding the six data (23 to 28) at lowest ΔH shown as diamonds that deviate from this linear relationship. The molar entropy ΔS is linearly related to the molar enthalpy ΔH

$$\Delta S = a + b\Delta H, \tag{8}$$

where $a=-327.5$ [J/(mol·K)] and $b=31.47\times10^{-4}$ (K^{-1}). The value of ΔH for breaking a single hydrogen bond is approximately 19×10^3 J/mol. Therefore, the value of ΔH for a thermal transition involving n hydrogen bonds being cooperatively broken is

$$\Delta H = n(19\times10^3\ \mathrm{J/mol}). \tag{9}$$

Along the x axis in Fig. 4 is a scale indicating the apparent number of hydrogen bonds (n) being cooperatively broken during the thermal transitions. The significance of the slope b is that $1/b$ denotes a special temperature, here called T_{eq}, at which any change in the number of hydrogen bonds causes balanced changes in the terms ΔH and $T_{eq}\Delta S$, such that the ΔG does not change. Hence the dynamics of the thermal transition do not depend on the number of hydrogen bonds. The value of T_{eq} can be expressed in degrees Celsius as T_{eq}

Table 1 Thermodynamc parameters for thermal transitions from literature.

No.	Thermal transition	Ref.	ΔS [J/(mol·K)]	ΔH (J/mol)
1	Monkey retinal damage	1	1652	6.276×10^5
2	Arterial tissue coagulation	2	974.8	4.300×10^5
3	Egg albumen whitening	3	856.7	3.849×10^5
4	Dog prostate whitening, scattering	4	−82.9	0.718×10^5
5	Dog prostate whitening, absorption	4	2.40	1.010×10^5
6	Necrosis of rat liver	5	392.3	2.219×10^5
7	Whitening of dog prostate	6,7	277.4	1.866×10^5
8	Whitening of dog heart	8	510.0	2.596×10^5
9	Whitening of pig liver	9	553.5	2.769×10^5
10	Contraction of mouse dermis	10	996.2	4.251×10^5
11	Collagen in lens capsule	11	2381	8.590×10^5
12	Rat tail collagen birefringence	12	831.2	3.676×10^5
13	Retinal coagulation	13	596.7	2.900×10^5
14	Retinal coagulation	14	991.7	4.200×10^5
15	Retinal coagulation	14	1764	6.700×10^5
16	Skin coagulation	15	1640	6.300×10^5
17	Pig kidney whitening	16	906.3	3.996×10^5
18	Pig kidney delayed necrosis	16	491.8	2.569×10^5
19	Induce heat shock protein	17	5169	17.40×10^5
20	Garlic allicin degradation	18	223.3	1.845×10^5
21	Bacteriochlorophyll dimer P	19	530.0	2.678×10^5
22	Bacteriochlorophyll dimer B	19	474.2	2.510×10^5
23	[a]Inactivation of L-DOPA synthesis	20	590.0	1.160×10^5
24	[a]Prostate BPH coag. (dye uptake)	21	214.7	0.401×10^5
25	[a]Prostate BPH coag. (histo)	21	192.7	0.384×10^5
26	[a]Ovalubumin denaturation (using DSC)	22	1252	0.053×10^5
27	[a]Kidney rf conductivity	23	420.2	0.570×10^5
28	[a]Kidney rf permittivity	23	305.4	0.480×10^5

[a]Denotes data shown as diamonds in Fig. 4. Other data shown as circles.

$=1/b-273.15$ and equals 44.6°C. The x intercept where ΔS equals 0 equals $-a/b$, which corresponds to 5.5 hydrogen bonds. Apparently each additional hydrogen bond starting with approximately the sixth bond begins to add order to the structure of biomolecules.

Figure 4 also showed six data (diamonds) at very low ΔH, which deviate from the linear relationship between ΔS and ΔH described above. These data, and other low-ΔH values in the literature that are not listed in Table 1, are quite variable,

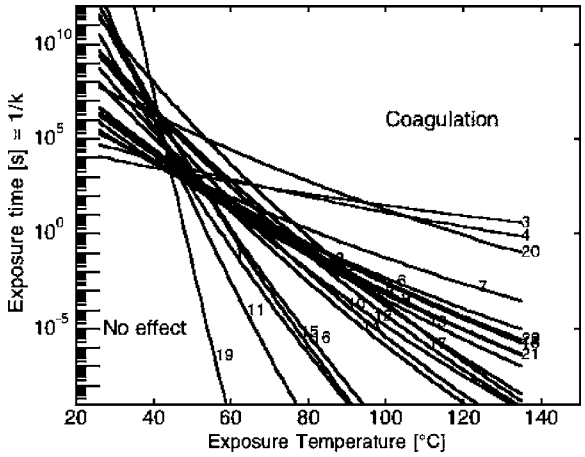

Fig. 3 Exposure time versus exposure temperature to achieve thermal damage for various types of transition (e.g., necrosis, whitening, dermal shrinkage, collagen birefringence loss) in various tissues. (Number labels refer to Table 1.)

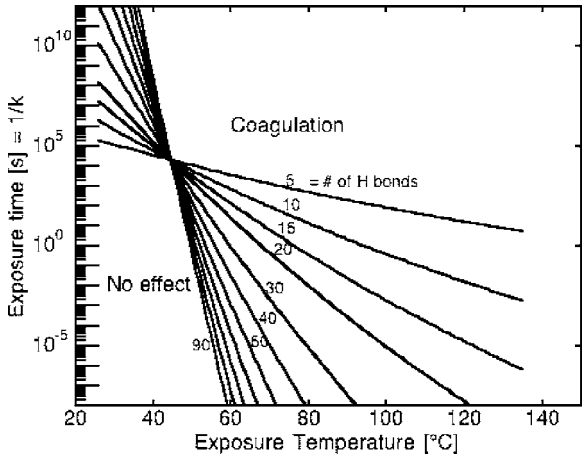

Fig. 5 Simulated relationship between ΔS and ΔH. Exposure time versus exposure temperature based on Eqs. (8) and (9) for a molecular structure held together by increasing numbers of hydrogen bonds, 5 to 90 bonds. Compare with Fig. 3.

which suggests that the first few bonds in a biomolecule provide an initial amount of order to the molecule, while the additional bonds, in the more ordered biomolecules involved in the high-ΔH transitions of Table 1, provide a fixed additional degree of order per added bond.

Figure 5 shows the predicted behavior of exposure time $[1/k(\mathrm{s})]$ versus exposure temperature $[T(°\mathrm{C})]$, as was seen in Fig. 3, for a varying number (n) of hydrogen bonds that must be cooperatively broken to allow the irreversible thermal transition. The curves illustrate how changing the number of hydrogen bonds (n) causes the curves to pivot around a point of constant exposure time (5.4 h) and exposure temperature $(T_{eq}=44.6°\mathrm{C})$, which achieves irreversible thermal transition regardless of the number of hydrogen bonds. Higher temperatures require shorter times for transition, and lower temperatures require longer times for transition, and the rates become dependent on the number of hydrogen bonds involved. The curves approximate the behavior of thermal transitions summarized in Fig. 3, but clearly there is variation in the experimental data.

For transitions involving 10, 20, and 30 hydrogen bonds, the threshold exposure times at 60 °C are 11 min, 24 s, and 867 ms, respectively. This may seem counterintuitive, because more bonds might be expected to further stabilize a biomolecule. However, added bonds increase both entropy and enthalpy, making the biomolecule behave more like a crystal with a sharp threshold melting temperature. At high temperatures, more bonds cause more rapid denaturation. The expected effect of more bonds is better seen at temperatures below $T_{eq}=44.6°\mathrm{C}$. For transitions involving 10, 20, and 30 hydrogen bonds, the threshold exposures at 43 °C are 7.8 h, 11 h, and 16 h, respectively. Now, the increase in bonds is indeed stabilizing the biomolecules.

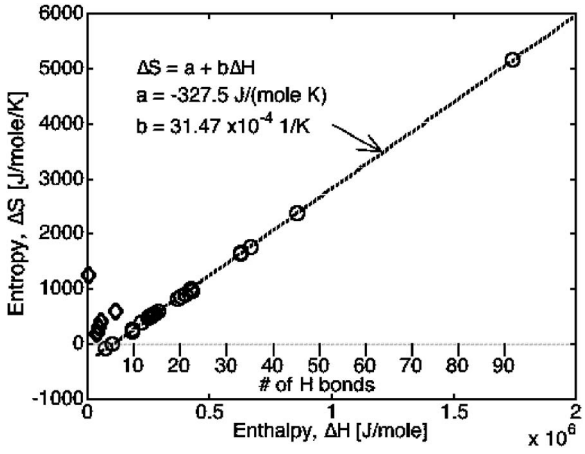

Fig. 4 Experimental relationship between ΔS and ΔH. Plot of molar entropy $\Delta S[\mathrm{J/(mol\cdot K)}]$ versus molar enthalpy ΔH (J/mol) for the examples of Fig. 3. The ΔS is linearly related to ΔH. Circles: data that conform to the linear relationship. Diamonds: data that deviate from the linear relationship.

5 Discussion

The fact that all the thermal transitions reported for tissue fall on a common line indicates a consistent increment in order per additional stabilizing bond, such that the ratio of $\Delta S/\Delta H$ for added bonds is constant. As a convenient convention, one can cite the equivalent number of cooperative hydrogen bonds involved in a thermal transition. This is only a convention, since other types of bonds (van der Waals, ionic, disulfide, covalent) may be involved yet yield the same $\Delta S/\Delta H$ ratio. So it should be emphasized that the tentative assignment of the cooperative bonds to hydrogen bonds is only a convention to provide an easily understood description. Then, only one independent parameter affects the rate of the thermal transition, that is, the apparent number of hydrogen bonds cooperatively breaking. Hydrogen bonds have a ΔH of about 19 kJ/mol. The slope of Fig. 4 suggests that the value of ΔS for breakage of a single hydrogen bond on average is $(19\ \mathrm{kJ/mol})(b)=59.8\ \mathrm{J/(mol\cdot K)}$. Therefore, the ΔS and ΔH observed for a particular thermal transition in a particular tissue can be summarized by the apparent number of hydrogen bonds being cooperatively broken, as indicated in Fig. 4.

Other factors may influence the $\Delta S/\Delta H$ ratio. For example, Wright et al.[24] discussed how axial tension applied to collagen fiber bundles in tendons increased the entropy of the denaturation, citing the early work of Weir[25] and the later work of Chen et al.[26] Miles et al.[27] reported that the effect of acetic acid on collagen molecule denaturation was to increase the $\Delta S/\Delta H$ ratio about 10%.

The simulations of Fig. 5 compare well with the experimental data of Fig. 3, suggesting that thermal coagulative transitions observed in biological tissues predominantly involve cooperative breakage of 10 to 90 equivalent hydrogen bonds, with most of the examples falling in the range of 10 to 20 hydrogen bonds.

The more hydrogen bonds involved in a thermal transition, the sharper the transition, in other words, the exposure temperature becomes more important than the exposure time. An example of a sharp transition would be the thermal changes in collagen of the lens [example 11 (Ref. 11)] which behaves as if ~45 hydrogen bonds are cooperatively broken. The less hydrogen bonds involved, the more horizontal is the transition and exposure time becomes more important and exposure temperature less important. An example of a more gradual transition would be the degradation of the allicin in garlic [example 20 (Ref. 18)] which behaves as if ~10 hydrogen bonds are cooperatively broken.

Of special interest is the thermal transition with the highest ΔH, example 19 (Ref. 17) in Table 1 and Fig. 3, which corresponds to the thermal transition that triggers the expression of the heat shock protein hsp-70. This transition appears to involve about 90 cooperative hydrogen bonds. The extremely high values of ΔH and ΔS yield a very sharp thermal transition, the most vertical curve in Fig. 3. When temperatures are just below T_{eq} (~44.6°C), the trigger for heat shock protein expression is the last transition to occur, the most resistant to thermal transition. When temperatures are just above T_{eq}, this trigger transition is the first transition to occur, the most rapid thermal transition. Therefore, the trigger hsp-70 expression would be one of the first thermal transitions to occur if a tissue is exposed to elevated temperatures. In other words, this transition may serve as a "sensor" for the onset of thermal damage that requires the protection afforded by increased heat shock protein expression. It is worth noting that the senior author of the Beckham et al. report, Jansen, trained as a graduate student with Welch.

Not all tissues operate with such a simple behavior. The simple first-order Arrhenius model of Eq. (1) would predict that a thermal transition proceeds to its final state regardless of the rate k involved (see Fig. 2). However, the optical changes in dog myocardium [example 8 (Ref. 7)] achieve a different final stable state dependent on the temperature used to achieve coagulation. Higher temperatures held for 2 h yielded higher final optical scattering. Lower temperatures held for 2 h yielded lower final optical scattering. Hence, there is a temperature-dependent path of coagulation. This is a complexity not considered in the simple Arrhenius model.

Another example of complexity is the optical change in pig liver during coagulation [example 9 (Ref. 8)]. The coagulative transitions begin 10-fold sooner and end 10-fold later than expected from the simple Arrhenius behavior shown in Fig. 2. (The data in Table 1 for this transition in liver used the midpoint of optical change to determine the ΔS and ΔH.) However, the final state of fully coagulated liver is the same regardless of the temperature used to achieve that change, in contrast to the dog myocardium behavior cited above. The liver's behavior is consistent with a distribution of rate constants k for a series of coagulative transitions, each with a different ΔS and ΔH and each contributing only a portion of the total optical change in scattering.

Note that the Arrhenius model predicts thermal damage will occur when tissues are exposed to a low temperature such as body temperature for a long time. The role of protein turnover and synthesis, cellular repair, and protective processes must be considered when long exposure times are involved. Theoretically, synthesis and repair could be treated as a replenishment of the native form of the biomolecules involved in the observed phenomenon. The protective processes, such as heat shock proteins, might be treated as a change in the apparent rate constant (k) for a transition.

Clearly, more work on thermal coagulation of tissues is warranted. This report hopefully provides a conceptual framework for predicting the expected behavior and guiding careful design of future experiments. Because photocoagulation is such a key application of lasers in medicine, our field of biomedical optics and laser interactions with cells and tissues would benefit from more work on thermal coagulation, following the early lead of Welch.

In summary, the convention of choosing the apparent number (n) of hydrogen bonds involved in a thermal transition specifies the ΔH, using Eq. (9). This ΔH value along with the parameters $a=-327.5$ J/(mol·K) and $b=31.47\times10^{-4}$ J/mol are inserted into Eq. (8) to specify the ΔS of the transition. This ΔH and ΔS are then used in Eq. (5) to predict the rate of transition, $k(\mathrm{s}^{-1})$, as a function of the exposure temperature. The threshold exposure time at constant exposure temperature equals $1/k(\mathrm{s})$. In this manner, the dynamics and energetics of irreversible thermal transitions involving cooperative breakage of bonds can be estimated. Such an estimate is generally applicable to a variety of thermal effects in biological tissues.

Acknowledgments

Deepest thanks to A.J. Welch for the attention, hospitality, and inspiration he provided me when I first began studying biomedical optics and laser interactions with cells and tissues.

References

1. A. J. Welch and G. D. Polhamus, "Measurement and prediction of thermal injury in the retina of the rhesus monkey," *IEEE Trans. Biomed. Eng.* **31**(10), 633–643 (1984).
2. Y. Yang, A. J. Welch, and H. G. Rylander III, "Rate process parameters of albumen," *Lasers Surg. Med.* **11**(2), 188–190 (1991).
3. R. Agah, J. A. Pearce, A. J. Welch, and M. Motamedi, "Rate process model for arterial tissue thermal damage: implications on vessel photocoagulation," *Lasers Surg. Med.* **15**(2), 176–184 (1993).
4. M. G. Skinner, S. Everts, A. G. Reid, I. A. Vitkin, L. Lilge, and M. D. Sherar, "Changes in optical properties of *ex vivo* rat prostate due to heating," *Phys. Med. Biol.* **45**, 1375–1386 (2000).
5. K. Matthewson, P. Coleridge-Smith, J. P. O'Sullivan, T. C. Northfield, and S. G. Bown, "Biological effects of intrahepatic neodymium: yttrium-aluminum-garnet laser photocoagulation in rats," *Gastroenterology* **93**(3), 550–557 (1987).
6. C. Newman and S. L. Jacques, University of Texas, M. D. Anderson Cancer Center, Personal communication (1991).

7. S. L. Jacques, M. Motamedi, and S. Rastegar, "Computer simulation of laser coagulation of prostate: a guide to dosimetry. American Society for Lasers in Medicine and Surgery, New Orleans, April 18–20, 1993," *Lasers Surg. Med.* **Suppl 5**, abstract 311 (1993).
8. S. L. Jacques and M. O. Gaeeni, "Thermally induced changes in optical properties of heart," *IEEE Eng. Med. Biol. Mag.* **11**(Part 4/6), 1199–1200 (1989).
9. S. L. Jacques, C. Newman, and X. Y. He, "Thermal coagulation of tissues: Liver studies indicate a distribution of rate parameters not a single rate parameter describes the coagulation process," *Proc. Annual Winter Meeting of the American Society of Mechanical Engineers*, Atlanta, GA (1991).
10. S. L. Jacques and S. A. Prahl, "Modeling optical and thermal distributions in tissue during laser irradiation," *Lasers Surg. Med.* **6**, 494–503 (1987).
11. C. A. Miles, "Kinetics of collagen denaturation in mammalian lens capsules studied by differential scanning calorimetry," *Int. J. Biol. Macromol.* **15**(5), 265–271 (1993).
12. D. J. Maitland and J. T. Walsh Jr., "Quantitative measurements of linear birefringence during heating of native collagen," *Lasers Surg. Med.* **20**, 310–318 (1997).
13. A. Vassiliadis, H. C. Christian, and K. G. Dedrick, "Ocular laser threshold investigations," *Aerosp. Med.* Report F41609-70-0002 (1971).
14. A. N. Takata, L. Zaneveld, and W. Richter, "Laser-induced thermal damage in skin," *Aerosp. Med.* Report F41609-70-0002 (1977); A. Vassiliadis, H. C. Christian, and K. G. Dedrick, "Ocular laser threshold investigations," *Aerosp. Med.* Report F41609-70-0002 (1977).
15. F. C. Henriques, "Studies of thermal injury. V: The predictability and the significance of thermally induced rate processes leading to irreversible epidermal injury," *Am. J. Pathol.* **23**, 489–502 (1947).
16. X. He, S. McGee, J. E. Coad, F. Schmidlin, P. A. Iaizzo, D. J. Swanlund, S. Kluge, E. Rudie, and J. C. Bischof, "Investigation of the thermal and tissue injury behaviour in microwave thermal therapy using a porcine kidney model," *Int. J. Hyperthermia* **20**(6), 567–593 (2004).
17. J. T. Beckham, M. A. Mackanos, C. Crooke, T. Takahashi, C. O'Connell-Rodwell, C. H. Contag, and E. D. Jansen, "Assessment of cellular response to thermal laser injury through bioluminescence imaging of heat shock protein 70," *Photochem. Photobiol.* **79**(1), 76–85 (2004).
18. P. Canizares, I. Gracia, L. A. Gomez, A. Garcia, C. Martin De Argila, D. Boixeda, and L. de Rafael, "Thermal degradation of allicin in garlic extracts and its implication on the inhibition of the *in-vitro* growth of Helicobacter pylori," *Biotechnol. Prog.* **20**(1), 32–37 (2004).
19. J. Tandori, Z. Tokaji, K. Misurda, and P. Maroti, "Thermodynamics of light-induced and thermal degradation of bacteriochlorins in reaction center protein of photosynthetic bacteria," *Photochem. Photobiol.* **81**(6), 1518-1525 (2005).
20. S. Ali, I. U. Haq, M. A. Qadeer, and M. I. Rajoka, "Double mutant of aspergillus oryzae for improved production of *L*-dopa (3,4-dihydroxyphenyl-L-alanine) from *L*-tyrosine," *Biotechnol. Appl. Biochem.* **42**(Pt 2), 143–149 (2005).
21. P. Bhowmick, J. E. Coad, S. Bhowmick, J. L. Pryor, T. Larson, J. De La Rosette, and J. C. Bischof, "In vitro assessment of the efficacy of thermal therapy in human benign prostatic hyperplasia," *Int. J. Hyperthermia* **20**(4), 421–439 (2004).
22. M. Weijers, P. A. Barneveld, M. A. Cohen Stuart, and R. W. Visschers, "Heat-induced denaturation and aggregation of ovalbumin at neutral pH described by irreversible first-order kinetics," *Protein Sci.* **12**(12), 2693–2703 (2003).
23. M. Pop, A. Molckovsky, L. Chin, M. C. Kolios, M. A. Jewett, and M. D. Sherar, "Changes in dielectric properties at 460 kHz of kidney and fat during heating: importance for radio-frequency thermal therapy," *Phys. Med. Biol.* **48**(15), 2509–2525 (2003).
24. N. T. Wright and J. D. Humphrey, "Denaturation of collagen via heating: An irreversible rate process," *Annu. Rev. Biomed. Eng.* **4**(1), 109–128 (2002).
25. C. E. Weir, "Rate of shrinkage of tendon collagen—heat, entropy, and free energy of activation of the shrinkage of untreated tendon. Effect of acid, salt, pickle, and tannage on the activation of tendon collagen," *J. Am. Leather Chem. Assoc.* **44**, 108–140 (1949).
26. S. S. Chen, N. T. Wright, and J. D. Humphrey, "Heat-induced changes in the mechanics of a collagenous tissue: isothermal isotonic shrinkage, *ASME J. Biomech. Eng.* **120**, 382–388 (1998).
27. C. A. Miles, T. V. Burjandadze, and A. J. Bailey, "The kinetics of the thermal denaturation of collagen in unrestrained rat tail tendon determined by differential scanning calorimetry," *J. Mol. Biol.* **245**, 437–446 (1995).